Systematic Analysis of $E(5)$ Critical-Point Nuclei in $A\sim130$ Region with Relativistic Mean Field Theory *

SHENG Zong-Qiang[1;1)] GUO Jian-You[2] MENG Ying[1]

1 (Department of Mathematics & Physics, Anhui University of Science and Technology, Huainan 232001, China)
2 (School of Physics & Material, Anhui University, Hefei 230039, China)

Abstract The shape phase transition between spherical $U(5)$ and γ-unstable $O(6)$ nuclei is investigated systemically for the nuclei in the $A\sim130$ region by the constrained relativistic mean field theory. By examining potential energy surfaces and neutron Fermi energies, we suggest that ^{136}Ba and ^{132,134}Xe are possible nuclei with $E(5)$ symmetry, which is favored by the observed ratio $R_{4/2}=(E^+_{41}-E^+_{01})/(E^+_{21}-E^+_{01})$. While the RMF predicted $E(5)$ symmetry for ^{128,130,132}Te cannot be supported by the observed ratio $R_{4/2}$. Whether these nuclei are critical-point nuclei should further be examined in experiments.

Key words relativistic mean field, $E(5)$ symmetry, critical-point nuclei, potential energy surfaces

1 Introduction

Critical-point symmetries in nuclear structure receive considerable attention recently. Many physical systems (nuclei, molecules, atomic clusters, etc.) are characterized by the shape in their equilibrium configuration. These shapes are rigid in many cases. However, in some cases the system is rather floppy. A challenging problem is how to describe the property of the phase transition point. In the original interacting boson model (IBM)[1], where nuclei are regarded as the systems composed of bosons with the $U(6)$ symmetry, one sees three dynamical symmetries $U(5)$, $SU(3)$ and $O(6)$, which geometrically correspond to the spherical vibration, the axially deformed rotation, and the γ-unstable rotation, respectively. In the IBM language, the symmetry $X(5)$ corresponds to the critical point between the $U(5)$ and $SU(3)$ symmetry limits while the symmetry $E(5)$ describes the region of the phase transition between the $U(5)$ and $O(6)$ dynamical symmetries. Thus, the $X(5)$ ($E(5)$) critical-point symmetry can be used to confirm the first- order (second-order) shape phase transition between the spherical nucleus and the axially deformed symmetric (γ-unstable) nucleus[2, 3].

The first identified nucleus with the $E(5)$ ($X(5)$) behavior was ^{134}Ba[4] (^{152}Sm)[5]. Systematic investigations suggested that ^{102}Pd, ^{106,108}Cd, ^{124}Te, and ^{128}Xe are closely related to the $E(5)$ critical-point model[6], while ^{126}Ba, ^{130}Ce, and the N=90 isotones of Nd, Sm, Gd, and Dy would demonstrate the $X(5)$ symmetry[7]. Additional examples can be found in the recent review articles on phase transitions in Ref. [8] and references therein. The $E(5)$ ($X(5)$) symmetry provides a classification of states and the analytic expression for the observables in the region where the nuclear structure changes most rapidly[9]. How to identify a nuclei which is close to the $E(5)$ ($X(5)$)

Received 4 September 2006, Revised 21 January 2007

* Supported by Natural Science Foundation of High Education of Anhui Province for Youths (2006jq1076), Natural Science Foundation of Anhui Educational Committee (2006KJ056C, 2006KJ259B), National Natural Science Foundation of China (10475001, 10675001), Program for New Century Excellent Talents in University of China (NCET-05-0558), and Program for Excellent Talents in Anhui Province University

1) E-mail: shengzongq309@yahoo.com.cn

symmetry is essential in better understanding the shape phase transition. Based on the Bohr-Mottelson collective model, the nuclei corresponding to the critical point of phase transition have been discussed by solving Bohr Hamiltonian with different potential shapes[10—16]. Recently, the relativistic mean field (RMF) theory has been applied to study the critical-point symmetry due to its success in describing a large amount of nuclear phenomena. The details can be found in the recent review articles and references therein[17, 18]. In Ref. [19], ^{148,150,152}Sm have been pointed out to be the possible critical-point nuclei with $X(5)$ symmetry by the RMF approach. We have systemically studied the rare-earth nuclei by using the RMF theory, and have predicted some critical-point nuclei, such as Ce[20], Nd, Gd and Dy isotopes[21]. In Ref. [22], the RMF theory with the NL3 force was used to obtain potential energy surfaces (PES) for a number of isotopes, which were suggested to have critical-point symmetries. It was shown that PES for the nuclei with the $E(5)$ symmetry is relatively flat, whereas for the nuclei with the $X(5)$ symmetry PES has a bump. However, more detailed information of the shape evolution for the nuclei in the $A\sim130$ region has not been studied in the framework of the RMF theory. In this paper, we examine potential energy surfaces and neutron Fermi energies, and compare those results with the experimental γ energy transition ratios so that we can predict $E(5)$ critical-point nuclei in the $A\sim130$ region.

2 The theoretical framework

To analyze critical-point nuclei by using the RMF theory, we first sketch the microscopic approach. In the framework of the RMF theory, the nuclear interaction is usually described by exchanging three mesons: the isoscalar-scalar meson σ, which supplies the medium-range attraction between nucleons, the isoscalar-vector meson ω^μ, which offers the short-range repulsion of the nucleon-nucleon interaction, and the isovector-vector meson $\boldsymbol{\rho}^\mu$, which provides the isospin dependence of the nuclear force. The effective Lagrangian density is the following

$$\begin{aligned}\mathscr{L} = {} & \bar{\psi}\left(\mathrm{i}\gamma^\mu\partial_\mu - M\right)\psi + \frac{1}{2}\partial^\mu\sigma\,\partial_\mu\sigma - \frac{1}{2}m_\sigma^2\sigma^2 - \\ & \frac{1}{3}g_2\sigma^3 - \frac{1}{4}g_3\sigma^4 - g_\sigma\bar{\psi}\sigma\psi - \frac{1}{4}W^{\mu\nu}W_{\mu\nu} + \\ & \frac{1}{2}m_\omega^2\omega^\mu\omega_\mu - g_\omega\bar{\psi}\gamma^\mu\omega_\mu\psi + \frac{1}{4}g_4\left(\omega^\mu\omega_\mu\right)^2 - \\ & \frac{1}{4}R^{\mu\nu}R_{\mu\nu} + \frac{1}{2}m_\rho^2\boldsymbol{\rho}^\mu\boldsymbol{\rho}_\mu - g_\rho\bar{\psi}\gamma^\mu\boldsymbol{\tau}\boldsymbol{\rho}_\mu\psi - \\ & \frac{1}{4}F^{\mu\nu}F_{\mu\nu} - e\bar{\psi}\gamma^\mu\frac{1-\tau_3}{2}A_\mu\psi\ . \end{aligned} \tag{1}$$

The classical variation principle leads to the Dirac equation

$$\left[-\mathrm{i}\alpha\cdot\nabla + V(\boldsymbol{r}) + \beta(M + S(\boldsymbol{r}))\right]\psi_i = \varepsilon_i\psi_i \tag{2}$$

for nucleon spinors and the Klein-Gordon equations

$$\begin{cases} (-\Delta + m_\sigma^2)\sigma(\boldsymbol{r}) = -g_\sigma\rho_{\mathrm{s}}(\boldsymbol{r}) - g_2\sigma^2(\boldsymbol{r}) - g_3\sigma^3(\boldsymbol{r}), \\ (-\Delta + m_\omega^2)\omega^\mu(\boldsymbol{r}) = g_\omega j^\mu(\boldsymbol{r}) - g_4(\omega^\nu\omega_\nu)\omega^\mu(\boldsymbol{r}), \\ (-\Delta + m_\rho^2)\boldsymbol{\rho}^\mu(\boldsymbol{r}) = g_\rho\boldsymbol{j}^\mu(\boldsymbol{r}), \\ -\Delta\,A^\mu(\boldsymbol{r}) = e j_{\mathrm{p}}^\mu(\boldsymbol{r}) \end{cases} \tag{3}$$

for mesons, where

$$\begin{cases} V(\boldsymbol{r}) = \beta\left[g_\omega\gamma^\mu\omega_\mu(\boldsymbol{r}) + g_\rho\gamma^\mu\boldsymbol{\tau}\boldsymbol{\rho}_\mu(\boldsymbol{r}) + e\gamma^\mu\frac{1-\tau_3}{2}A_\mu(\boldsymbol{r})\right], \\ S(\boldsymbol{r}) = g_\sigma\sigma(\boldsymbol{r}) \end{cases} \tag{4}$$

are the vector and scalar potentials, respectively.

The Eqs. (2) and (3) can self-consistently be solved by iteration. The details can be found in Refs. [23, 24]. The binding energy at certain deformation value is obtained by constraining the quadrupole moment $\langle Q_2\rangle$ to a given value μ_2 in the expectation value of the Hamiltonian[25]

$$\langle H'\rangle = \langle H\rangle + \frac{1}{2}C_\mu\left(\langle Q_2\rangle - \mu_2\right)^2\ , \tag{5}$$

where C_μ is the constraint factor. The deformation parameter β_2 is obtained from the calculated quadrupole moments $\langle Q_2\rangle$ for the proton and the neutron through

$$\langle Q_2\rangle = \langle Q_{2\mathrm{p}}\rangle + \langle Q_{2\mathrm{n}}\rangle = \frac{3}{\sqrt{5\pi}}A\,R_0^2\,\beta_2 \tag{6}$$

with $R_0 = 1.2A^{1/3}$.

3 Numerical details and results

For the nuclei studied in this paper, full N=14 deformed harmonic oscillator shells are taken into account and very good convergency for the resultant binding energy and deformation is obtained. The converged deformation corresponding to different μ_2 values is not sensitive to the deformation parameter β_0 of the harmonic oscillator basis in a reasonable range because a large basis is used. Different choices of β_0 will lead to different iteration circles in the self-consistent calculation and different computational time. But physical quantities such as the binding energy and the deformation do not change much. Thus the deformation parameter β_0 of the harmonic oscillator basis can be chosen near the expected deformation so that the higher accuracy and shorter computation time can be achieved. By varying the μ_2 value, the binding energy at different deformations can be obtained. The pairing effect is considered by the constant gap approximation (BCS) in which the pairing gap is taken as $11.2/\sqrt{A}$ for even number nucleons.

The binding energies and the quadrupole deformations for the ground states in the constrained RMF theory with the PK1[26] parameter set are tabulated in Table 1. Calculations with the NL3[27] and TMA[28] parameter sets are also performed. The results which do not depend on the effective interactions are not presented here. For binding energies, the data are well reproduced within a deviation of 0.5%. Particularly for ^{122}Te, the difference between the RMF results and the data is less than 0.175MeV. For deformations, tendencies of shape curves with respect to the neutron number in the Ba and Xe isotopes are correctly reproduced in the RMF calculations. Although there is a little underestimation for neutron-riched nuclei, the obtained deformations considerably agree with the experimental data, especially for the nuclei near the stable-line. For Te isotopes, the oblate shapes are predicted in the RMF calculation, which seem to be in disagreement with the experimental data. Comparing with the fact that the prolate or oblate shapes cannot be distinguished experimentally, the RMF calculation with the assumption of the oblate shape can correctly reproduce the data of $^{120—128}$Te.

Table 1. Experimental data[29, 30] and resultant ground state binding energy $E_{\rm B}$ and quadrupole deformation β_2 for Ba, Xe and Te isotopes obtained in the constrained RMF calculations with the PK1 interaction.

Nucl.	$E_{\rm B}$/MeV		Nucl.	$E_{\rm B}$/MeV		Nucl.	$E_{\rm B}$/MeV	
	Expt.	Cal.		Expt.	Cal.		Expt.	Cal.
^{124}Ba	1036.127	1036.958	^{122}Xe	1027.640	1028.289	^{120}Te	1017.280	1017.539
^{126}Ba	1055.850	1056.730	^{124}Xe	1046.254	1047.035	^{122}Te	1034.330	1033.155
^{128}Ba	1074.727	1076.144	^{126}Xe	1062.913	1064.960	^{124}Te	1050.684	1049.157
^{130}Ba	1092.731	1094.581	^{128}Xe	1080.743	1082.084	^{126}Te	1066.374	1066.038
^{132}Ba	1110.042	1112.404	^{130}Xe	1096.906	1098.289	^{128}Te	1081.440	1081.301
^{134}Ba	1126.700	1129.748	^{132}Xe	1114.447	1114.205	^{130}Te	1095.942	1096.181
^{136}Ba	1142.781	1146.710	^{134}Xe	1127.434	1129.900	^{132}Te	1109.942	1111.420
^{138}Ba	1158.298	1164.212	^{136}Xe	1141.877	1145.685	^{134}Te	1123.270	1125.841
Nucl.	β_2		Nucl.	β_2		Nucl.	β_2	
	Expt.	Cal.		Expt.	Cal.		Expt.	Cal.
^{124}Ba	0.302	0.297	^{122}Xe	0.259	0.241	^{120}Te	0.201	−0.177
^{126}Ba	0.279	0.256	^{124}Xe	0.212	0.219	^{122}Te	0.185	−0.175
^{128}Ba	0.249	0.218	^{126}Xe	0.188	0.198	^{124}Te	0.170	−0.152
^{130}Ba	0.218	0.180	^{128}Xe	0.184	0.176	^{126}Te	0.153	−0.131
^{132}Ba	0.186	0.142	^{130}Xe	0.169	0.152	^{128}Te	0.136	−0.112
^{134}Ba	0.161	0.115	^{132}Xe	0.141	0.113	^{130}Te	0.118	0.088
^{136}Ba	0.126	0.071	^{134}Xe	0.119	0.071	^{132}Te	**	0.033
^{138}Ba	0.090	0.000	^{136}Xe	0.122	0.000	^{134}Te	**	0.000

Due to the success in describing ground state properties, we apply the RMF theory to the study of the nuclear shape phase transition. The resultant potential energy curves for $^{124-138}$Ba, $^{122-136}$Xe, $^{120-134}$Te in the constrained RMF calculations with the PK1 effective interaction are plotted in Figs. 1, 2 and 3, respectively. In each figure, the energy of the ground state is taken as a reference.

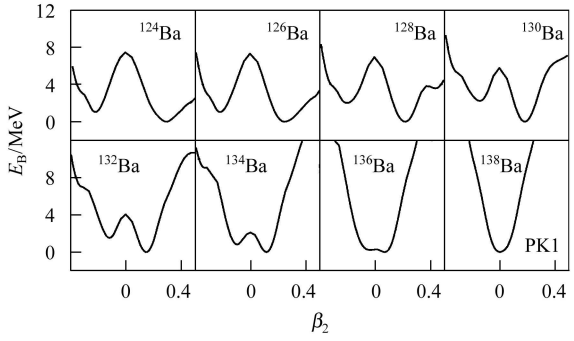

Fig. 1. The potential energy surfaces for Ba isotopes obtained in the constrained RMF calculation with the PK1 interaction. While the ground state binding energy is taken as a reference.

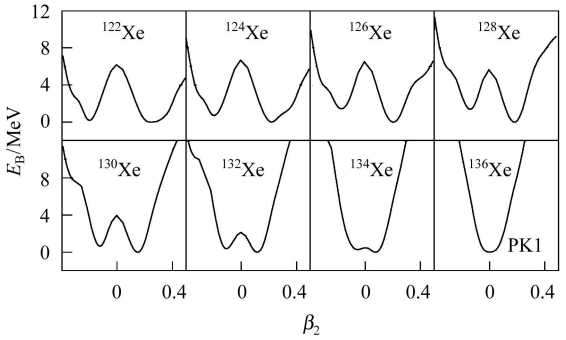

Fig. 2. The same as Fig. 1, but for Xe isotopes.

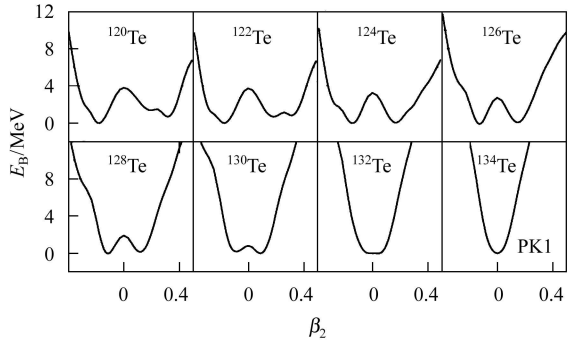

Fig. 3. The same as Fig. 1, but for Te isotopes.

It is found that the ground state of ^{138}Ba is in the spherical shape and has a stiff barrier of over 17MeV with increasing deformation. PES of ^{136}Ba is quite flat around β_2=0.00. Comparing with ^{136}Ba, PES of ^{134}Ba is less flat, and is symmetric around β_2=0.00 (from β_2=−0.15 to β_2=0.15), i.e., non-axially symmetric deformation from $\gamma=0°$ to $\gamma=60°$. It implies that ^{134}Ba might be a γ-unstable nucleus. With this indication, as emphasized in Ref. [22] that the relatively flat PES is the character of the critical-point symmetry $E(5)$, ^{136}Ba whose character situates between the vibration mode and the γ-unstable behavior is a possible candidate with the $E(5)$ symmetry. Starting from ^{132}Ba, with decreasing neutron number, the ground state gradually changes to the deformed form and the potential energy curve becomes softer, and finally reaches to well deformed $^{124-130}$Ba. The same calculations are also performed for Xe and Te isotopes. The corresponding PES' are shown in Figs. 2 and 3, respectively. Similar to the analysis for Ba isotopes, we suggest that ^{132,134}Xe and ^{128,130,132}Te are the candidates of critical-point nuclei with the $E(5)$ symmetry, respectively.

One of the merits of microscopic nuclear models such as RMF theory is that it can provide detailed information on single particle levels, shell structure, and Fermi energy etc., which are very important for us to discuss nuclear structure and to examine the deformation induced effect. In Fig. 4, the neutron Fermi energies for $^{124-138}$Ba, $^{122-136}$Xe, and $^{120-134}$Te are demonstrated. These results are calculated with the effective interaction PK1. Similar single-particle structures can be obtained by employing two other effective interactions, and thus will not be presented here.

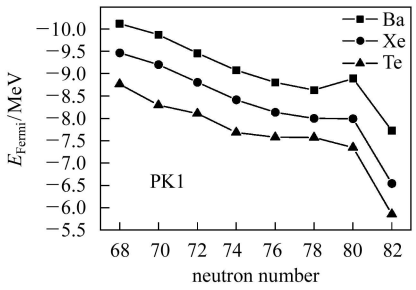

Fig. 4. Neutron Fermi energies for Ba, Xe and Te isotopes in the constrained RMF calculations with the PK1 interaction.

From Fig. 4, a monotonic decreasing behavior of neutron Fermi energy with increasing neutron num-

ber is seen for Ba, Xe, Te isotopes till N=78. After N=78, the change of the Fermi energy appears unusual. Fermi energy in ^{136}Ba increases unconventionally, while in ^{138}Ba, it decreases dramatically. This suggests that the phase transition might occur in N=80, i.e., ^{136}Ba might be a critical-point nucleus with the $E(5)$ behavior. The same phenomena are also found for Xe and Te isotopes, which implies that ^{132,134}Xe and ^{128,130,132}Te are possible critical-point nuclei with the $E(5)$ symmetry, which agrees with the PES analysis.

To confirm the theoretical predictions, the ratios of experimental excitation energies as well as corresponding characteristic ratios $R_{4/2}$ $=(E^+_{41}-E^+_{01})/(E^+_{21}-E^+_{01})$ for Ba, Xe, and Te isotopes are listed in Table 2.

Table 2. The experimental values[31] of $R_{4/2}$ for Ba, Xe and Te isotopes.

Nucl.	$R_{4/2}$	Nucl.	$R_{4/2}$	Nucl.	$R_{4/2}$
^{124}Ba	2.83	^{122}Xe	2.50	^{120}Te	2.07
^{126}Ba	2.78	^{124}Xe	2.48	^{122}Te	2.09
^{128}Ba	2.68	^{126}Xe	2.42	^{124}Te	2.07
^{130}Ba	2.52	^{128}Xe	2.33	^{126}Te	2.04
^{132}Ba	2.43	^{130}Xe	2.25	^{128}Te	2.01
^{134}Ba	2.32	^{132}Xe	2.16	^{130}Te	1.94
^{136}Ba	2.28	^{134}Xe	2.04	^{132}Te	1.72
^{138}Ba	1.31	^{136}Xe	1.29	^{134}Te	1.23

From Table 2, one sees that the experimental data for ^{132,134,136}Ba are in agreement with the predictions mentioned above. Especially for ^{136}Ba, the observed ratio $R_{4/2}$=2.28 is located almost exactly at the middle point between the mode of harmonic vibration with $U(5)$ symmetry ($R_{4/2}$=2.00) and the mode of γ-unstable rotation with $O(6)$ symmetry ($R_{4/2}$=2.50). In addition, the $U(5)$ limit nucleus ^{138}Ba is correctly predicted, which is in agreement with the data of $R_{4/2}$=1.31 with a bit non-collective behavior. In particular, the well deformed nuclei $^{124-130}$Ba predicted by the RMF theory are supported by the experiment data by comparing with the $SU(3)$ limit value of $R_{4/2}$=3.33. All these show that RMF calculations can satisfactorily reproduce the experimental data available. Therefore, the $E(5)$ symmetry for ^{134}Ba predicted by RMF might be reasonable and should be checked in the experiment.

For Xe isotopes, the observed ratio shows that $^{124-134}$Xe whose behaviors situate between the spherical ($R_{4/2}$=2.00) and the γ-unstable behaviors ($R_{4/2}$=2.50) are possible critical-point nuclei with the $E(5)$ symmetry. This again agrees with the analyses on PES and the Fermi energy. While for Te isotopes, all the observed ratios are smaller than 2.2, which implies that the predicated Te isotopes with the $E(5)$ symmetry are not favored by the experimental $R_{4/2}$ data. Whether ^{128,130,132}Te are the nuclei with the $E(5)$ symmetry should further be examined in the experiment.

4 Conclusion

The shape phase transition from the spherical $U(5)$ to the γ-unstable $O(6)$ symmetries for the nuclei in the $A\sim 130$ region is systemically investigated by the constrained relativistic mean field theory. The experimental data for the properties of the ground states of Ba, Xe and Te isotopes are fairly well described. By examining nuclear potential energy surfaces and Fermi energies, ^{136}Ba and ^{132,134}Xe are suggested to be the possible nuclei with the $E(5)$ symmetry, which is favored by the observed ratio $R_{4/2}=(E^+_{41}-E^+_{01})/(E^+_{21}-E^+_{01})$. While predicted ^{128,130,132}Te with the $E(5)$ symmetry are not supported by the observed ratio $R_{4/2}$, which should further be examined in the experiment.

References

1 Iachello F, Arima A. The Interacting Boson Model. Cambridge: Cambridge University Press, 1987
2 Iachello F. Phys. Rev. Lett., 2001, **87**: 052502
3 Iachello F. Phys. Rev. Lett., 2000, **85**: 3580
4 Casten R F, Zamfir N V. Phys. Rev. Lett., 2000, **85**: 3584
5 Casten R F, Zamfir N V. Phys. Rev. Lett., 2001, **87**: 052503
6 Clark R M, Cromaz M, Deleplanque M A et al. Phys. Rev., 2004, **C69**: 064322
7 Clark R M, Cromaz M, Deleplanque M A et al. Phys. Rev., 2003, **C68**: 037301
8 Dennis Bonatsos. Phase Transitions: Summary of Discussion Session II of Camerino 2005, xxx.lanl.gov, nucl-th/0512091, 2005
9 Leviatan A, Ginocchio J N. Phys. Rev. Lett., 2003, **90**: 212501
10 Caprio M A. Phys. Rev., 2004, **C69**: 044307
11 Bonatsos D, Lenis D, Minkov N et al. Phys. Rev., 2004, **C69**: 014302
12 Bonatsos D, Lenis D, Minkov N et al. Phys. Rev., 2004, **C70**: 024305
13 Bonatsos D, Lenis D, Minkov N et al. Phys. Lett., 2004, **B584**: 40
14 Dusling K, Pietralla N. Phys. Rev., 2005, **C72**: 011303
15 Bizzeti P G, Bizzeti-Sona A M. Eur. Phys. J., 2004, **A20**: 179; Phys. Rev., 2004, **C70**: 064319
16 Fortunato L. Eur. Phys. J., 2005, **A26**(Supplement 1): 1
17 Vretenar D, Afanasjev A V, Lalazissis G A et al. Physics Reports, 2005, **409**: 101
18 MENG J, Toki H, ZHOU S G et al. Progress in Particle and Nuclear Physics, 2006, **57**: 470
19 MENG J, ZHANG W, ZHOU S G et al. Eur. Phys. J., 2005, **A25**: 23
20 YU M, ZHANG P F, RUAN T N et al. Int. J. Mod. Phys., 2006, **E15**: 939
21 SHENG Z Q, GUO J Y. Mod. Phys. Lett., 2005, **A20**: 2711
22 Fossion R, Bonatsos D, Lalazissis1 G A. Phys. Rev., 2006, **C73**: 044310
23 Gambhir Y, Ring P, Thimet A. Ann. Phys. (N.Y.), 1990, **198**: 132
24 ZHOU S G, MENG J, Ring P. Phys. Rev., 2003, **C68**: 034323
25 Ring P, Schuck P. The Nuclear Many Body Problem. Springer, 1980
26 LONG W H, MENG J, Giai N V et al. Phys. Rev., 2004, **C69**: 034319
27 Lalazissis G A, König J, Ring P. Phys. Rev., 1997, **C55**: 540
28 Sugahara Y. PhD Thesis, Tokyo Metropolitan University, 1994
29 Audi G, Wapstra A H. Nucl. Phys., 1995, **A595**: 409
30 Raman S, Nestor C W, Tikkanen P. Jr. At. Data Nucl. Data Tables, 2001, **78**: 1
31 Nuclear Data Sheets, as of June 2005

相对论平均场理论对 $A\sim130$ 区 $E(5)$ 关键点核的研究*

圣宗强[1;1)]　郭建友[2]　孟影[1]

1 (安徽理工大学数理系　淮南　232001)
2 (安徽大学物理与材料科学学院　合肥　230039)

摘要　利用形变约束的相对论平均场理论系统地研究了 $A\sim130$ 区 Ba, Xe 和 Te 同位素偶–偶核的基态性质, 理论计算数据和实验数据符合得非常好. 详细分析了这些核的位能曲面、费米能和 γ 跃迁能量的分支比, 给出了 ^{136}Ba, ^{132,134}Xe 具有 $E(5)$ 对称性的预言. 对于 ^{128,130,132}Te 这 3 个核, 理论计算的结果表明其具有 $E(5)$ 对称性, 但 γ 跃迁能量的分支比的实验值不支持理论结果. 此 3 个核是否为关键点核有待于实验的进一步检验.

关键词　相对论平均场　$E(5)$ 对称性　关键点核　位能曲面

2006 – 09 – 04 收稿,　2007 – 01 – 21 收修改稿

∗ 安徽省高校青年教师自然科学基金 (2006jq1076), 安徽省教育厅自然科学基金 (2006KJ056C, 2006KJ259B), 国家自然科学基金 (10475001, 10675001), 教育部新世纪优秀人才支持计划基金 (NCET-05-0558) 和安徽省高等学校拔尖人才基金资助

1) E-mail: shengzongq309@yahoo.com.cn